J Nanostruct 16(3): 3337-3345, Summer 2026

RESEARCH PAPER

Green-Synthesized Silver Nanoparticles: Cytotoxic Effects on MDA-MB-231 and MCF-7 Cancer Cell Lines and Physicochemical Characterization

Abualfadhel Yahya T.* *, Jenan Hussein Taha, Ibramim Abdullah Mahmood

Department of Physiology and Medical Physics, College of Medicine, Al-Nahrain University, Baghdad, Iraq

ARTICLE INFO

Article History:
Received 13 March 2026
Accepted 18 May 2026
Published 01 July 2026

Keywords:
Beetroot
Breast Cancer
Cytotoxicity
Green Synthesis
Nanoparticles
Silver Nanoparticles

ABSTRACT

The application of nanotechnology in cancer therapy has attracted significant attention in recent years. Among various nanomaterials, silver nanoparticles (AgNPs) have demonstrated promising potential due to their relatively low toxicity toward normal cells, cost-effectiveness, and potential ability to selectively target cancer cells. This study aimed to evaluate the inhibitory biological activity of silver nanoparticles against two human breast cancer cell lines, MCF-7 and MDA-MB-231. Silver nanoparticles were characterized using several analytical techniques including X-ray Diffraction (XRD), Ultraviolet-Visible Spectroscopy (UV-VIS), Energy Dispersion X-ray (EDX), Atomic Force Microscopy (AFM), and Filed Emission Scanning Electron Microscopy (FE-SEM). The characterization results confirmed the successful synthesis of quasi-spherical silver nanoparticles with particle sizes ranging from 30 to 40 nm. The cytotoxic effect of the synthesized AgNPs was investigated using the MTT assay on both MCF-7 and MDA-MB-231 cell lines at six different concentrations. The results indicated a concentration-dependent inhibitory effect of silver nanoparticles on both cancer cell lines, with a stronger cytotoxic activity observed against the MDA-MB-231 cell line. These findings highlight the potential of silver nanoparticles as promising anticancer agents against breast cancer cells and support the need for further investigations using more advanced biological models.

How to cite this article
Yahya A., Hussein Taha J., Abdullah Mahmood I. Green-Synthesized Silver Nanoparticles: Cytotoxic Effects on MDA-MB-231 and MCF-7 Cancer Cell Lines and Physicochemical Characterization. J Nanostruct, 2026; 16(3):3337-3345. DOI: 10.22052/JNS.2026.03.027

INTRODUCTION

Nanotechnology has attracted the attention of researchers due to its excellent physical, chemical, and mechanical properties, which increase its potential applications in numerous fields. The applications of each material vary depending on its mechanical properties (size, shape, and strength), chemical properties (chemical stability), and physical properties (dimensions) [1-3]. Furthermore, the properties of nanomaterials vary depending on the synthesis method, which in turn affects the size, shape, and structure of the nanoparticles [4,5]. Synthesizing nanoparticles from plants in more than one way. Nanoparticles can be synthesized from within plant cells, from outside plant cells, or using plant extracts. Plant-based nanoparticle synthesis is possible

* *Corresponding Author Email:*
abulfadhel.y.tuama.mphy24@ced.nahrainuniv.edu.iq

due to the presence of proteins, carbohydrate complexes, amino acids, aldehydes, and other biomolecules. Plant extracts act as reducing and stabilizing agents for nanoparticles, but the degree of reduction or stabilization varies due to the differences in the biological components, which lead to variations in the size and shape of the nanoparticle crystals [6,7]. Beetroot extract contributes to the reduction of silver ions due to its content of chemical compounds such as flavonoids [8], triterpenes [9], and betalains [10], which contribute to the reduction of silver ions efficiently and safely [8]. Silver nanoparticles differ from other nanoparticles in their common and diverse uses, due to their distinctive properties such as crystal structure and crystal arrangement, in addition to optical and catalytic properties [11]. Although silver nanoparticles have numerous industrial and biosensor applications, but one of their most important current applications is in biology. This is due to the declining effectiveness of antibiotics and the development of bacterial defense systems [12]. When silver is reduced to the nanoscale (1–100 nm), it exhibits behaviors that differ markedly from its bulk form, including enhanced surface reactivity, strong antimicrobial activity, and distinctive optical phenomena arising from localized surface plasmon resonance (LSPR) [13]. Due to the fact that silver nanoparticles possess a sustained ability to resist and combat bacterial and fungal cells, making them a key nanomaterial for coating medical devices to maintain sterility. These silver nanoparticles act as an antibacterial and antifungal barrier by continuously liberation silver ions, thus preventing microbial growth [14]. There is warned against using certain forms of silver nanoparticles (such as nanowires and nanorods) in medical or sterilization applications due to their significant cytotoxicity to normal cells. Also spherical silver nanoparticles are completely safe to interact with normal cells [15]. The use of nanoparticles in general, and silver nanoparticles in particular, has expanded in cancer treatment due to their low toxicity to normal cells, low cost compared to their high efficacy, and the ability to target nanomaterials specifically to cancer cells [16]. Silver nanoparticles synthesized through green synthesis were more toxic against cancer cells. For example, the Moringa oleifera leaves extract used in the synthesis of silver nanoparticles increased the therapeutic effect of the silver nanoparticles in liver cancer cells, acute lymphoblastic leukemia, and myeloid leukemia [17]. Silver nanoparticles interact with cancer cells. This interaction occurs through the ability of silver nanoparticles to penetrate the cell membrane, increasing the concentration of Reactive Oxygen Species (ROS), which leads to cellular oxidation and consequently programmed cell death (apoptosis). Alternatively, silver nanoparticles may directly attack the cell's powerhouses (mitochondrion), also leading to cell death, or they may damage the cell's DNA, rendering it incapable of replication. While all of these processes are possible, silver nanoparticles typically act through one of these methods [18]. Silver nanoparticles have selective behavior of cells as we explained previously, silver nanoparticles increase the percentage of reactive oxygen species (ROS) in abnormal or non-human cells, but in normal cells, they decrease the percentage of ROS. They also contribute to activating cell proliferation by helping to increase the secretion of some types of cytokines [19].

Therefore, this study aims to evaluate the biological effect of silver nanoparticles synthesized by green synthesis against the MCF-7&MDA-MB-231 cell line, in addition to studying the structural, optical and morphological properties of the silver nanoparticles synthesized by green synthesis.

MATERIALS AND METHOD

Preparation of Plant Extract

beetroot were purchased from local markets and soaked in deionized water to remove all soil and impurities. After an hour, the outer crust of the beetroot was removed with a sharp knife and soaked again in deionized water for an hour to completely remove the soil and impurities. The beetroot were then cut into equal-sized rings 5 mm to 10 mm thick and dried for 6.5 to 7 hours using a fruit dryer. After ensuring that the slices were completely dry, they were ground and sifted to obtain a homogeneous powder. We took 30 grams of the powder and added it to 250 ml of deionized water for 2 hours. The water was then filtered through sterile gauze, and to ensure that the water did not contain any impurities Finally, the mixture was filtered using chromatography paper [20].

Preparation of Silver Nanoparticles

One gram of silver nitrate ($AgNO_3$) was dissolved in 100 ml of deionized water. At the

same time, one gram of citric acid($C_6H_8O_7$) was dissolved in 200 ml of beetroot extract. Next, 50 ml of the silver nitrate($AgNO_3$) solution was added to 200 ml of beetroot extract in which one gram of citric acid($C_6H_8O_7$) had been dissolved. The solution was stored at room temperature in a dark place for 6 hours. After this period, the solution was centrifuged at 8000 rpm for half an hour, and the precipitate was washed with deionized water (this process was repeated five times). After washing, the solution was dried in a thermal oven at 80 °C for 6 hours. The dried precipitate was re-incinerated in a high-temperature oven at 500 °C for 2 hours to obtain a highly crystalline powder and remove most of the organic materials used in the preparation method.

Methyl Thiazolyl Tetrazolium (MTT) assay
Culture the Cell on a Cytotoxicity Plate

The cytotoxicity plate is cultured by taking 150 ml of the culture medium for the cell line located at the Biotechnology Research Center - Al-Nahrain University/Baghdad/Iraq for each well in the plate and keeping it in an autoclave for 24 hours at a temperature of 37°C.

Dissolve Nanoparticles with Cancer Cells

The concentrations are divided for interaction with cancer cell lines by dissolving 10 mg of silver nanoparticles in 4 mL of deionized water to obtain a 100% concentration, dissolving 5 mg of silver nanoparticles in 4 mL of deionized water to obtain a second concentration (50%), and dissolving 2.5 mg, 1.25 mg, 0.625 mg, and 0.3125 mg of silver nanoparticles in the same way, thus obtaining six different concentrations of silver nanoparticles. Then, 100 µL of each concentration is taken and added to six wells in a cytotoxicity plate for interaction with cancer cells and incubated in autoclave for 24 hours at 37°C.

Toxicity Assay Investigation

To determine the percentage of biological inhibition of silver nanoparticles on the last day, we add 10 microliters of MTT dye to each well in a cytotoxicity plate and incubate it for 2 to 4 hours until we observe a color change in each well. The plate is then read using an ELISA analyzer, and Eqs. 1 and 2 are used to analyze the ELISA data.

$$\text{Viability} = \frac{\text{Optical Density of Concentration}}{\text{Optical Density of Control}} \times 100\% \quad (1)$$

$$\text{Inhibition rate} = \text{Viability} - 100 \quad (2)$$

RESULTS AND DISCUSSION

X-Ray Diffraction for Silver Nanoparticles (AgNPs)

The X-ray diffraction pattern of silver

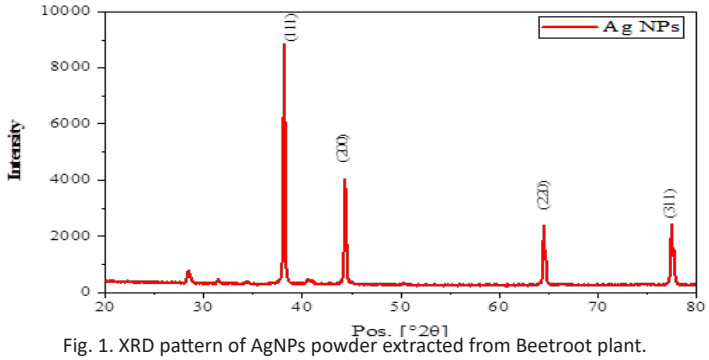

Fig. 1. XRD pattern of AgNPs powder extracted from Beetroot plant.

Table 1. Identification Parameters of AG NPs Obtained from XRD Results.

Pos. [°2θ]	FWHM [°2θ]	Crystallite Size [nm]	Micro Strain [%]
38.1122	0.1537	74.9	0.15744
44.3119	0.1662	64.0	0.15962
64.5152	0.1587	78.5	0.09198
77.5077	0.1827	68.7	0.08956

nanoparticles prepared using beetroot extract shows characteristic diffraction peaks of at angles 2Θ ≈ 38.11°, 44.31°, 64.52°, 77.51°, 81.67°, and 98.08°, which can be assigned to the crystalline planes (111), (200), (220), (311), (222), and (040), as in Fig. 1 respectively, perfectly corresponding to the face-centered cubic (FCC) phase of metallic silver (Ag).

In addition to the main peaks, weak peaks were observed at lower angles, such as 2Θ≈ 28.41°, 31.40°, 34.34°, 40.63°, 50.30°, 66.48°, and 68.99°, which do not represent secondary crystalline phases.

Crystal size and microscopic stress of nanoparticles were calculated using the Depay-Shearer equation, depending on the breadth of the main peaks in the XRD pattern of the Cubic Faceted Cubic Phase (FCC), and as illustrated in Table 1.

Ultra Vault – Visible Spectrum (UV-Vis Spectrum) for Silver Nanoparticles (AgNPs)

The UV-Vis absorption spectrum of silver nanoparticles prepared by green synthesis shows the absence of the expected sharp plasmonic peak for silver nanoparticles at around 420–430 nm, with the appearance of a clear peak in the visible region at around 551 nm as in Fig. 2.

In addition, the exponential absorption tail was analyzed using the normalized logarithm curve of the absorption coefficient ln(α) versus the photon energy hv. The curve showed a clear linear region in the low-energy range between 1.2 and 2.3 eV, which was used to extract the Urbach EU energy through a precise linear fit. The extracted Urbach EU energy was approximately

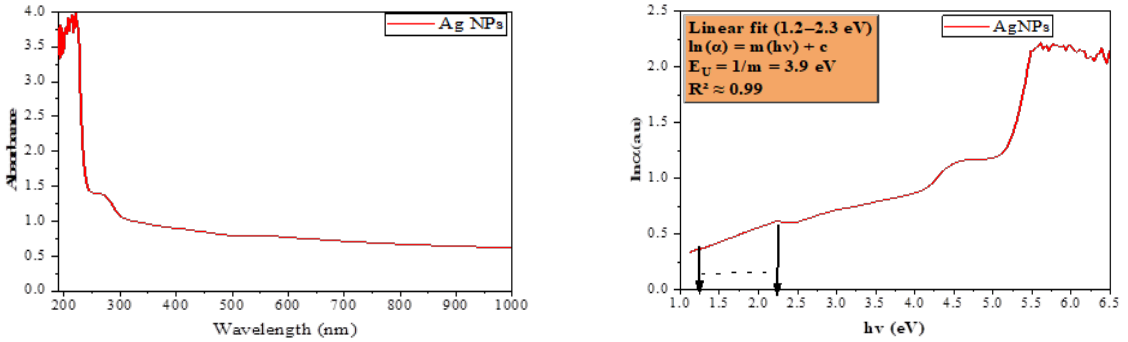

Fig. 2. Absorption spectra of AgNPs powder extracted from Beetroot plant and Urbach energy of AgNPs powder extracted from Beetroot Plant.

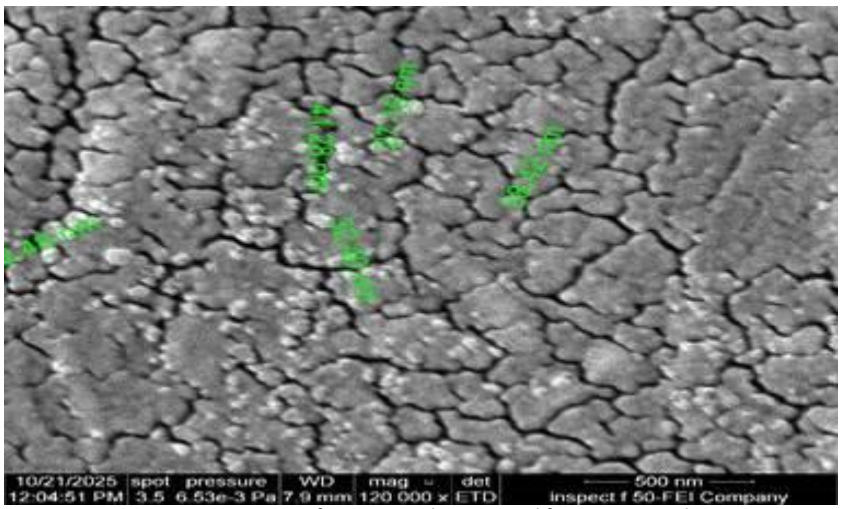

Fig. 3. FE-SEM image of AgNPs powder extracted from Beetroot plant.

3.9 eV, a relatively high value reflecting significant electronic disorder and localized states resulting from structural inhomogeneity and the small size of the nanoparticles as in Fig. 3.

Field Emission-Scanning Electron Microscopy (FE-SEM) for Silver Nanoparticles (AgNPs)

The Field Emission Scanning Electron Microscopy (FE-SEM) image of silver nanoparticles prepared using beetroot extract shows an irregular surface structure composed of closely packed and partially agglomerated nanoparticles with a relatively heterogeneous size distribution. The particles appear as dense granular aggregates with indistinct boundaries, and the measured sizes fall within the nanoscale, with approximate particle diameters ranging from about 30 nm to 40 nm, as illustrated in the Fig. 3.

Energy Dispersive X-Ray (EDX) for Silver Nanoparticles (AgNPs)

The EDX spectrum showed distinct and strong peaks for silver at energies close to 3 keV, confirming the chemical composition of the formed particles, while the absence of strong peaks for other exotic elements indicates relatively good particle purity.

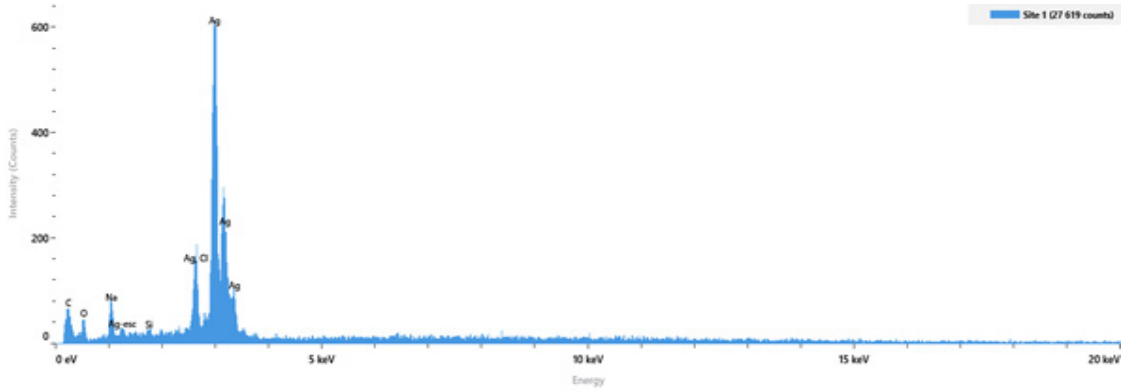

Fig. 4. EDX spectra of AgNPs powder extracted from Beetroot plant.

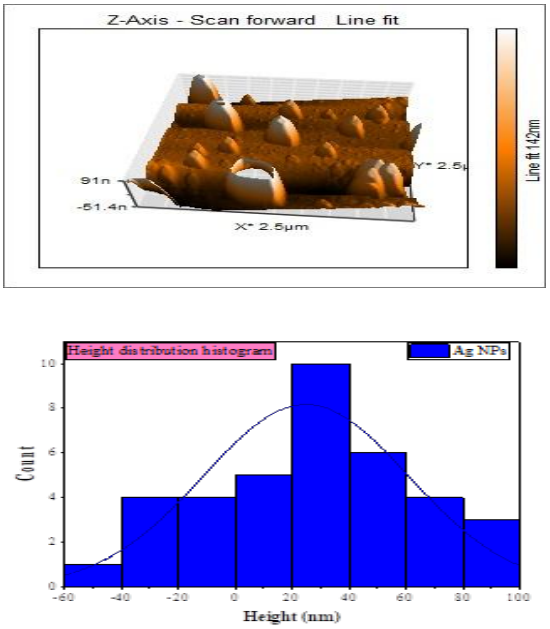

Fig. 5. AFM Image and cumulation distribution of AgNPs powder extracted from Beetroot Plant.

The appearance of weak secondary peaks for elements such as C, O, Na, and Cl also suggests this as in Fig. 4.

Atomic Force Microscopy (AFM) for Silver Nanoparticles (AgNPs)

Area roughness data showed that the average surface roughness Sa ≈ 20.11 nm, while the root square roughness value Sq ≈ 30.67 nm, and the maximum values for height and depression (Sp ≈ 143.07 nm and Sv ≈ −68.19 nm) and total height Sy ≈ 211.26 nm. As for the line roughness level, values of Ra ≈ 4.52 nm and Rq ≈ 6.76 nm were recorded, with a peak-drought difference Ry ≈ 40.00 nm and that is can be shown in Fig. 5.

Cytotoxicity Test for Silver Nanoparticles (AgNPs)

Six concentrations of silver nanoparticles were tested on two types of cancer cell lines: MDA-MB-231 (triple-negative cancer cell) and MCF-7 (triple-positive cancer cell). The results showed that the highest concentration of silver nanoparticles (2.5 mg/ml) inhibited 60.61% of the MDA-MB-231 cell line, while the inhibition rate of the same concentration of silver nanoparticles decreased to 14.828% when tested on the MCF-7 cell line. The second concentration (1.25 mg/ml) also had the ability to inhibit 58.70% of MDA-MB-231 cell lines, and the same concentration inhibited 12.759% of MCF-7 cell lines, and the remaining concentration illustrated in Fig. 6.

X-Ray Diffraction (XRD) for Silver Nanoparticles (AgNPs)

The Mellor coefficients (111), (200), (220), (311), (222), and (400), respectively, confirmed the face-centered cubic (FCC) crystalline phase of metallic silver (Ag), thus confirming the success of the bioreduction of silver ions and the formation of highly crystalline silver nanoparticles. The (111) peak exhibited the highest intensity, indicating a preferential trend toward crystal growth, a behavior common in nanoparticles prepared using green methods, this agreement with [21].

The angles 2θ ≈ 34.34°, 40.63°, and 68.99°, which do not represent secondary crystalline phases, these can be attributed to the Cu Kβ radiation effect from the X-ray source, especially if a nickel filter (Ni filter) was not used or Kβ stripping was not applied during data processing, this agreement with [22]. In addition to the angles 2θ ≈ 28.41°, 31.40°, 50.30°, and 66.48°, which are likely due to trace amounts of plant extract components and residual salts from the reaction medium, this agreement with [23]. It is noteworthy that the intensity of these peaks is very low compared to the main peaks, indicating that metallic silver remains the clearly dominant phase. The variation in crystal size and microstress values between different crystalline levels reflects the directional

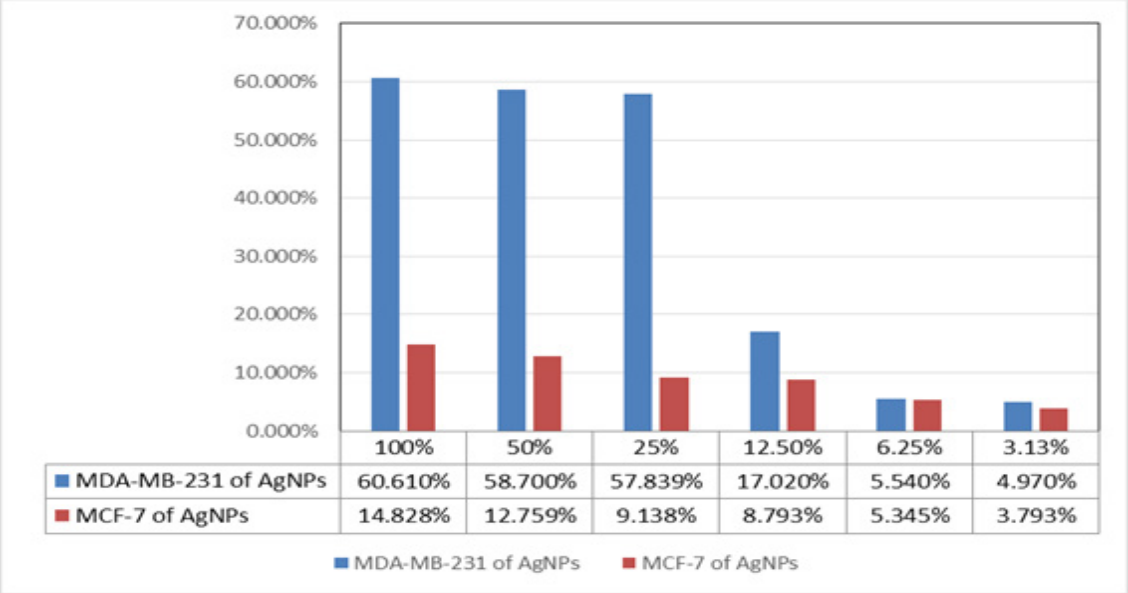

	100%	50%	25%	12.50%	6.25%	3.13%
MDA-MB-231 of AgNPs	60.610%	58.700%	57.839%	17.020%	5.540%	4.970%
MCF-7 of AgNPs	14.828%	12.759%	9.138%	8.793%	5.345%	3.793%

Fig. 6. Cytotoxicity of AgNPs against cancer cell.

nature of crystal growth (anisotropic growth) and the influence of surface defects and lattice distortions associated with the green synthesis and organic encapsulation of silver nanoparticles, this agreement with [24]. Based on the above, it can be concluded that the XRD pattern confirms the formation of silver nanoparticles.

Ultra Vault – Visible Spectrum (UV-Vis Spectrum) for Silver Nanoparticles (AgNPs)

This optical behavior of the absorption spectrum of silver nanoparticles is attributed to the superposition of several overlapping factors. The strong absorbance background of the organic compounds active in the beetroot extract, particularly the plant pigments and phenolic compounds, raises the baseline and obscures the original plasmonic peak. Furthermore, the presence of a broad size distribution of nanoparticles, with the potential for the formation of particles with relatively larger diameters, leads to a broadening of the surface plasmon resonance range and a shift towards longer wavelengths.

The appearance of a peak at 551 nm is indicative of partial nanoparticle aggregation, where plasmonic coupling between closely spaced particles results in a redshift of the plasmonic response and the appearance of an additional absorption component in the visible region. The plasmonic effects of the silver particles are intertwined with the organic adsorption of the plant extract and with the morphological factors of the particles, which is agreement with [25].

The increase in EU corresponds to a broadening of the SPR response and its extension to longer wavelengths, where increased surface disorder and plasmonic damping weaken the sharp plasmonic peak and reveal broad absorption components in the visible region. Since silver is a metallic material that does not possess a true energy gap, the extracted Urbach energy does not represent a conventional energy gap tail as in semiconductors, but rather an effective optical parameter (Urbach-like parameter) that describes the degree of electronic disorder and surface interactions in the greensynthetic silver nanoparticles, this agreement with [26].

Field Emission-Scanning Electron Microscopy (FE-SEM) for Silver Nanoparticles (AgNPs)

The morphological behavior of silver nanoparticles is attributed to the dual role of bioactive compounds present in beetroot extract. These compounds act as both reducing agents for silver ions and stabilizing agents, limiting excessive crystalline growth of the particles. However, this can also lead to partial aggregation resulting from surface interactions and hydrogen bonding between the organically coated particles. A relatively rough surface texture is observed, indicating a high specific surface area, which directly impacts the optical and plasmonic properties of the nanoparticles. The heterogeneous size distribution and partial aggregation result in a broad surface plasmon resonance response and the absence of a sharp plasmon peak, this agreement with [27].

Energy Dispersive X-Ray (EDX) for Silver Nanoparticles (AgNPs)

The presence of C, O, Na, and Cl is attributed to bioactive organic compounds remaining from the plant extract, which play a dual role as both a reducing agent and a stabilizer for nanoparticles, thus supporting the mechanism of green synthesis, this agreement with [28]. Elemental mapping obtained from EDX analysis also confirmed the uniform distribution of silver particles on the sample surface, with no significant variation in chemical composition.

Table 2. Elemental compositions weight% and atomic% of AgNPs Powder Extracted from Beetroot Plant.

Element	Atomic %	Weight %
C	23.3	6.2
O	38.0	13.4
Cl	7.3	5.7
Ag	31.5	74.8

Atomic Force Microscopy (AFM) for Silver Nanoparticles (AgNPs)

The surface roughness and mean surface roughness data indicate a marked height variation due to the distribution and partial aggregation of nanoparticles on the surface. Furthermore, the extreme height and depression values provide evidence of prominent nano-protrusions representing areas of concentration or aggregation of silver particles, contrasted with low-lying areas representing interstitial spaces or a thin organic layer resulting from plant compounds acting as reducing and stabilizing agents.

The linear roughness data also provided evidence of relative uniformity of the sample surface on linear sections, with the influence of nanoparticles remaining evident.

These results are consistent with (FE-SEM) images, which showed quasi-spherical nanoparticles with a limited tendency to aggregate, and with (XRD) results, which confirmed the nanocrystalline nature of the silver. Functionally, the increased surface roughness and formation of nano-protrusions contribute to enhancing the concentration of the local electromagnetic field, which directly strengthens the (SPR) phenomenon observed in UV-Vis spectra, making the prepared silver nanoparticles suitable for advanced sensing, optical, and catalytic applications.

Cytotoxicity Test for Silver Nanoparticles (AgNPs)

The results of the cytotoxicity tests for silver nanoparticles against cancer cell lines indicated a very significant difference in cytotoxicity, with MDA-MB-231 cells exhibiting greater responsiveness to the therapeutic effects of silver nanoparticles.

The resistance of MCF-7 cells can be attributed to their possession of defense mechanisms that reduce the oxidative stress induced by silver nanoparticles. These cells have the ability to release proteins (GSH and SOD) that contribute to reducing oxidative stress caused by silver nanoparticles. In contrast, MDA-MB-231 cells lack the same ability to synthesize these proteins due to significant DNA abnormalities, this agreement with [29].

Furthermore, MCF-7 cells have a cell membrane reinforced with membrane proteins that reduce the possibility of nanoparticle entry into the cell, and in some cases, at low concentrations, may even prevent nanoparticle entry. MDA-MB-231 cells, lack this property due to their rapid cell division, thus facilitating the entry of nanoparticles into the cell this agreement with [29].

In addition, MCF-7 cells possess the ability to expel nanoparticles from the cell via cellular expulsion pumps that distinguish between nutrient and toxic compounds, whereas MDA-MB-231 cells lack these defense systems, this agreement with [30].

CONCLUSION

In conclusion, silver nanoparticles (AgNPs) were successfully synthesized through an environmentally friendly green synthesis approach using beetroot extract as a natural reducing and stabilizing agent. Structural characterization by XRD confirmed the formation of highly crystalline face-centered cubic silver nanoparticles, while FE-SEM and AFM analyses revealed nanoscale particles with partial aggregation and heterogeneous morphology. EDX analysis further verified the high purity and uniform elemental distribution of silver within the prepared samples. Optical investigations demonstrated broad visible-light absorption with a red-shifted plasmonic response, attributed to nanoparticle aggregation, surface disorder, and interactions with phytochemical compounds from beetroot extract. The elevated Urbach-like energy indicated significant electronic disorder associated with nanoscale effects and organic surface encapsulation. Biological evaluation showed that the synthesized AgNPs exhibited selective cytotoxic activity against breast cancer cell lines, with markedly higher inhibition efficiency toward MDA-MB-231 cells compared with MCF-7 cells. This selective behavior is associated with differences in oxidative stress resistance, membrane permeability, and intracellular defense mechanisms between the two cell types. Overall, the obtained results demonstrate that beetroot-mediated AgNPs possess promising structural, optical, and anticancer properties, highlighting their potential for future biomedical, therapeutic, sensing, and nanotechnological applications.

CONFLICT OF INTEREST

The authors declare that there is no conflict of interests regarding the publication of this manuscript.

REFERENCES

1. Khan Y, Sadia H, Ali Shah S, Khan M, Shah A, Ullah N, et al.

Classification, Synthetic, and Characterization Approaches to Nanoparticles, and Their Applications in Various Fields of Nanotechnology: A Review. Catalysts. 2022;12(11):1386.
2. Burlec AF, Corciova A, Boev M, Batir-Marin D, Mircea C, Cioanca O, et al. Current Overview of Metal Nanoparticles' Synthesis, Characterization, and Biomedical Applications, with a Focus on Silver and Gold Nanoparticles. Pharmaceuticals. 2023;16(10):1410.
3. Taha JH, Abbas NK, Al-Attraqchi AAF. Green Synthesis and Evaluation of Copper Oxide Nanoparticles using Fig Leaves and their Antifungal and Antibacterial Activities. International Journal of Drug Delivery Technology. 2020;10(03):378-382.
4. Duman H, Eker F, Akdaşçi E, Witkowska AM, Bechelany M, Karav S. Silver Nanoparticles: A Comprehensive Review of Synthesis Methods and Chemical and Physical Properties. Nanomaterials. 2024;14(18):1527.
5. Hussein Taha J. Synthesis, characterization of $Ca(OH)_2$:TiO_2 nanocomposite and evaluation of its antimicrobial efficacy. Biomedicine. 2023;43(5):1496-1501.
6. Eweis AA, El-Raheem HA, Ahmad MS, Hozzein WN, Mahmoud R. Green Fabrication of Nanomaterials Using Microorganisms as Nano-Factories. J Cluster Sci. 2024;35(7):2149-2176.
7. Hano C, Abbasi BH. Plant-Based Green Synthesis of Nanoparticles: Production, Characterization and Applications. Biomolecules. 2021;12(1):31.
8. Nakashima T, Uetake J, Segawa T, Procházková L, Tsushima A, Takeuchi N. Spatial and Temporal Variations in Pigment and Species Compositions of Snow Algae on Mt. Tateyama in Toyama Prefecture, Japan. Frontiers in Plant Science. 2021;12.
9. Ermi Hikmawanti NP, Fatmawati S, Asri AW. The Effect of Ethanol Concentrations as The Extraction Solvent on Antioxidant Activity of Katuk (Sauropus androgynus (L.) Merr.) Leaves Extracts. IOP Conference Series: Earth and Environmental Science. 2021;755(1):012060.
10. Kauffmann AC, Castro VS. Phenolic Compounds in Bacterial Inactivation: A Perspective from Brazil. Antibiotics. 2023;12(4):645.
11. Abbas R, Luo J, Qi X, Naz A, Khan IA, Liu H, et al. Silver Nanoparticles: Synthesis, Structure, Properties and Applications. Nanomaterials. 2024;14(17):1425.
12. Khalifa HO, Oreiby A, Mohammed T, Abdelhamid MAA, Sholkamy EN, Hashem H, et al. Silver nanoparticles as next-generation antimicrobial agents: mechanisms, challenges, and innovations against multidrug-resistant bacteria. Frontiers in Cellular and Infection Microbiology. 2025;15.
13. Layth Mohammed Abbas Al M, Isam Abdulmunem A, Alaa Mohammed Abbas Al M. Optimization The Utility Of E-Learning Platform Through Integrating Smart Emotional Recognition Feature. Jornual of AL-Farabi for Engineering Sciences. 2022;1(2):6.
14. Shewale MM, Mali KK, Jatte KP, Marale PS. Silver Nanoparticles as Broad-Spectrum Antimicrobial Agents: Applications, Challenges, and Future Directions in Microbial Control. International Journal of Drug Delivery Technology. 2025;15(01).
15. Marassi V, Di Cristo L, Smith SGJ, Ortelli S, Blosi M, Costa AL, et al. Silver nanoparticles as a medical device in healthcare settings: a five-step approach for candidate screening of coating agents. Royal Society Open Science. 2018;5(1):171113.
16. Verma K, Bhattu M, Verma K, Kumar S, Kathuria D. Advances in plant-based nanomaterials for targeted Cancer therapy: Advances, mechanistic insights, and future prospects (2018–2022). Inorg Chem Commun. 2025;182:115351.
17. Srisaisap M, Boonserm P. Anticancer efficacy of biosynthesized silver nanoparticles loaded with recombinant truncated parasporin-2 protein. Sci Rep. 2024;14(1).
18. Ammar MM, Ali R, Abd Elaziz NA, Habib H, Abbas FM, Yassin MT, et al. Nanotechnology in oncology: advances in biosynthesis, drug delivery, and theranostics. Discover Oncology. 2025;16(1).
19. Kaya M, Akdaşçi E, Eker F, Bechelany M, Karav S. Recent Advances of Silver Nanoparticles in Wound Healing: Evaluation of In Vivo and In Vitro Studies. Int J Mol Sci. 2025;26(20):9889.
20. Kaba B, Zannou O, Ali Redha A, Koca I. Enhancing extraction of betalains from beetroot (Beta vulgaris L.) using deep eutectic solvents: optimization, bioaccessibility and stability. Food Production, Processing and Nutrition. 2024;6(1).
21. Labulo AH, David OA, Terna AD. Green synthesis and characterization of silver nanoparticles using Morinda lucida leaf extract and evaluation of its antioxidant and antimicrobial activity. Chemical Papers. 2022;76(12):7313-7325.
22. Stojilovic N. Using Cu Kα1/Kα2 Splitting and a Powder XRD System To Discuss X-ray Generation. J Chem Educ. 2018;95(4):598-600.
23. Izak-Nau E, Huk A, Reidy B, Uggerud H, Vadset M, Eiden S, et al. Impact of storage conditions and storage time on silver nanoparticles' physicochemical properties and implications for their biological effects. RSC Advances. 2015;5(102):84172-84185.
24. Asif M, Yasmin R, Asif R, Ambreen A, Mustafa M, Umbreen S. Green Synthesis of Silver Nanoparticles (AgNPs), Structural Characterization, and their Antibacterial Potential. Dose-Response. 2022;20(2).
25. Rai M, Yadav A, Gade A. Silver nanoparticles as a new generation of antimicrobials. Biotechnol Adv. 2009;27(1):76-83.
26. Wang C, Zhuang D, Zhao M, Li Y, Dong L, Wang H, et al. Effects of silver-doping on properties of Cu(In,Ga)Se2 films prepared by CuInGa precursors. Journal of Energy Chemistry. 2022;66:218-225.
27. Alavi M. Review of: "Nanoengineering of eco-friendly silver nanoparticles using five different plant extracts and development of cost-effective phenol nanosensor". Qeios Ltd; 2021. http://dx.doi.org/10.32388/7a02d9
28. Ramzan M, Abusalah M, Ahmed N, Yean C, Zeshan B. Green Synthesis and Characterization of Silver Nanoparticles Using Zingiber officinale Extracts to Investigate Their Antibacterial Potential. International Journal of Nanomedicine. 2024;Volume 19:13319-13338.
29. Theodossiou TA, Ali M, Grigalavicius M, Grallert B, Dillard P, Schink KO, et al. Simultaneous defeat of MCF7 and MDA-MB-231 resistances by a hypericin PDT–tamoxifen hybrid therapy. npj Breast Cancer. 2019;5(1).
30. Musielak M, Boś-Liedke A, Piwocka O, Kowalska K, Markiewicz R, Lorenz A, et al. Methodological and Cellular Factors Affecting the Magnitude of Breast Cancer and Normal Cell Radiosensitization Using Gold Nanoparticles. International Journal of Nanomedicine. 2023;Volume 18:3825-3850.